This is a repository copy of *Combination of electron energy-loss spectroscopy and energy dispersive x-ray spectroscopy to determine indium concentration in InGaN thin film structures*.

White Rose Research Online URL for this paper:
http://eprints.whiterose.ac.uk/91480/

Version: Accepted Version

Article:

Wang, X., Chauvat, M.P., Ruterana, P. et al. (1 more author) (2015) Combination of electron energy-loss spectroscopy and energy dispersive x-ray spectroscopy to determine indium concentration in InGaN thin film structures. Semiconductor Science and Technology, 30 (11). 114011. ISSN 0268-1242

https://doi.org/10.1088/0268-1242/30/11/114011

Reuse
Unless indicated otherwise, fulltext items are protected by copyright with all rights reserved. The copyright exception in section 29 of the Copyright, Designs and Patents Act 1988 allows the making of a single copy solely for the purpose of non-commercial research or private study within the limits of fair dealing. The publisher or other rights-holder may allow further reproduction and re-use of this version - refer to the White Rose Research Online record for this item. Where records identify the publisher as the copyright holder, users can verify any specific terms of use on the publisher’s website.

Takedown
If you consider content in White Rose Research Online to be in breach of UK law, please notify us by emailing eprints@whiterose.ac.uk including the URL of the record and the reason for the withdrawal request.

eprints@whiterose.ac.uk
https://eprints.whiterose.ac.uk/

1
2
3
4
5
6
7
8
9
10
11
12
13
14
15
16
17
18
19
20
21
22
23
24
25
26
27
28
29
30
31
32
33
34
35
36
37
38
39
40
41
42
43
44
45
46
47
48
49
50
51
52
53
54
55
56
57
58
59
60

Combination of electron energy-loss spectroscopy and energy dispersive X-ray spectroscopy to determine indium concentration in InGaN thin film structures

X Wang[1], MP Chauvat[2], P Ruterana[2] and T Walther[1*]

[1]Department of Electronic and Electrical Engineering, University of Sheffield, Mappin Building, Mappin Street, Sheffield S1 3JD, UK
[2]CIMAP, UMR 6252, CNRS-ENSICAEN-CEA-UCBN, 14050 Caen, cedex, France

*Email: t.walther@sheffield.ac.uk

Abstract: We demonstrate a method to determine the indium concentration, *x*, of $In_xGa_{1-x}N$ thin films by combining plasmon excitation studies in electron energy-loss spectroscopy (EELS) with a novel way of quantification of the intensity of X-ray lines in energy-dispersive X-ray spectroscopy (EDXS). The plasmon peak in EELS of InGaN is relatively broad. We fitted a Lorentz function to the main plasmon peak to suppress noise and the influence from the neighbouring Ga 3d transition in the spectrum, which improves the precision in the evaluation of the plasmon peak position. As the indium concentration of InGaN is difficult to control during high temperature growth due to partial In desorption, the nominal indium concentrations provided by the growers were not considered reliable. The indium concentration obtained from EDXS quantification using Oxford Instrument ISIS 300 X-ray standard quantification software often did not agree with the nominal indium concentration, and quantification using K and L lines was inconsistent. We therefore developed a self-consistent iterative procedure to determine the In content from thickness-dependent *k*-factors using, as described in recent work submitted to Journal of Microscopy. When the plasmon peak position is plotted versus the indium concentration from EDXS we obtain a linear relationship over the whole compositional range, and the standard error from linear

1
2
3
4
5
6
7
8
9
10
11
12
13
14
15
16
17
18
19
20
21
22
23
24
25
26
27
28
29
30
31
32
33
34
35
36
37
38
39
40
41
42
43
44
45
46
47
48
49
50
51
52
53
54
55
56
57
58
59
60

least-squares fitting shows that the indium concentration can be determined from the plasmon peak position to within $\Delta x = \pm 0.037$ standard deviation.

1. Introduction

III-V nitride semiconductor materials have great potential for optoelectronics due to their direct and adjustable band-gap and their relative insensitivity to dislocations [1]. During the past decade, several types of Light Emitting Diodes (LED) and Laser Diodes (LD) have been fabricated based on $In_xGa_{1-x}N$ quantum wells or nanowires [2, 3]. Wurtzite structure GaN and InN have direct band-gaps of 3.4eV and 0.7eV, respectively, so $In_xGa_{1-x}N$ compounds cover the band-gap range from 0.7eV to 3.4eV, which includes emission wavelengths corresponding to red, green and blue light. As the indium concentration changes, a morphological instability may be induced during growth of nanowires [3] or thin films. In order to clarify the effect of indium concentration on growth and optical properties, a reliable and highly accurate determination of indium concentration in $In_xGa_{1-x}N$ will be required.

As Narukawa *et al.* [4] suggested in 1997, transmission electron microscopy (TEM) and energy dispersive X-ray spectroscopy (EDXS) techniques can be used to determine the localization of excitons at deep traps originating from In-rich regions in the quantum wells [5], however, due to the image observed in TEM being essentially a result of averaging through the thickness of the sample, a quantitative determination of the indium composition is difficult to obtain from conventional TEM [2]. In order to solve this problem, we have combined a self-consistent iterative procedure developed for EDXS in TEM with plasmon energy measurements by electron energy-loss spectroscopy (EELS). As the scattering cross-section for plasmon scattering is much higher than that for ionization core-losses (K, L or M), our EELS experiments could be conducted at dose levels sufficiently low to neglect beam-induced changes of the In/Ga ratio in InGaN. In [3] such studies have already been performed, however, mostly confined to the compositional range $0 \leq x \leq 0.5$.

2. Experimental

2.1 $In_xGa_{1-x}N$ thin film growth

The investigated InGaN samples have been grown by metalorganic vapour phase epitaxy (MOVPE) in a close-couple shower head AIXTRON reactor using trimethyl-gallium (TMGa), trimethyl-indium (TMIn) for the metals and NH_3 for nitrogen. Three important parameters have been particularly investigated and monitored for the control of the indium incorporation: growth temperature, chamber pressure and III/V ratio. The growth of highest indium content layers has been carried out at the lowest temperature of 550°C, as well as highest III/V ratio (>40000). For the layers with In composition below 25%, the growth temperature could be above 700°C. The nominal indium concentration was first assessed by high resolution X-ray diffraction (XRD). For TEM investigation, cross-sectional specimens were prepared by conventional grinding and dimpling, followed by ion milling. In order to minimize the ion beam damage, the samples were maintained at liquid nitrogen temperature during ion milling using a Gatan PIPS at 5 keV, with a final polishing step at 0.6 keV. During the whole procedure, the beam angle was set at 5° for the two guns. Prior to analytical TEM by EDXS and EELS, conventional TEM investigations were performed by high resolution TEM using a JEOL 2010

1
2
3 microscope, for defect investigation in order to determine the strain relaxation mechanisms in
4 these layers which may involve the formation of typical defects such as dislocations [6, 7, 8],
5 stacking faults [9, 10, 11] and, in the worst cases, inversion domains [12, 13] as well as phase
6 ordering and phase separation [14, 15].
7
8
9
10 *2.2 EDXS and EELS characterization*
11 Analytical TEM was carried out on a Schottky field-emission JEOL 2010F transmission
12 electron microscope operated at 197kV (this voltage allows the user to increase the high
13 tension by up to 3kV for energy-filtered imaging, cf. [16]). The microscope is equipped with a
14 Gatan Imaging Filter (GIF 200) that allows for an energy resolution of ~0.9 eV, measured as
15 the full width at half-maximum (FWHM) of the zero-loss peak (ZLP). All spectra were
16 collected in diffraction mode with a collection semi-angle of ~20 mrad using a dispersion of
17 0.0502eV per channel (calibrated by drift tube offsetting), ~5nA beam current and ~50nm
18 probe size to avoid electron beam damage of the sample. Several spectra were recorded for
19 each thin film sample, from different regions of different specimen thickness. At this high
20 dispersion, the spectrometer dispersion is constant over the whole field of view, as confirmed
21 earlier by others [17], and drift of the high tension or the magnetic prism strength is not a
22 problem as the zero loss is recorded within all low loss spectra and it is only the distance of
23 the plasmon peak from the zero loss peak that matters.
24 For EDXS, an Oxford Instruments Si:Li detector with ultrathin window and the slowest pulse
25 processor settings in the ISIS300 software package were used. The energy resolution of the
26 EDXS system depends on the X-ray energy as well as on the pulse processor settings and
27 varies between 60eV (FWHM of strobe) and 136eV (FWHM of Mn Kα at 5895eV). In some
28 cases, a Cu signal was observed due to the copper support, however, this did not influence
29 quantification. Care was taken to avoid strong diffraction conditions that are known to
30 influence the X-ray yields, particularly near zone-axis and two-beam conditions [18]. Tilting
31 the layers by a few degrees off the zone axis while keeping them almost edge-on does not
32 cause a problem as long as the beam (~50nm diameter) remains well contained within the
33 layers (>80nm thick).
34
35
36
37 **3. Result and Discussion**
38 A typical low loss EEL spectrum of an $In_xGa_{1-x}N$ thin film is shown in Fig 1. Two main
39 features are observed: the zero-loss peak and the bulk plasmon excitation. The plasmon peak
40 position has been used to determine the Al concentration in $Al_xGa_{1-x}N$ thin film samples [19,
41 20] and the In concentration in $In_xGa_{1-x}N$ [3]. For the latter, however, no calibration points for
42 the range $0.5<x<1$ were available, so the quality of the linear fit proposed therein could be
43 questioned.
44 For determining the plasmon peak energy highly accurately, Fourier logarithm deconvolution
45 should be applied to remove the plural scattering [21]. Figure 1(a) shows the comparison of
46 original low loss EELS and deconvoluted spectra of an $In_{0.54}Ga_{0.46}N$ thin film. The
47 deconvolution method changes the height of the plasmon peaks but has no effect on the
48 plasmon peak energy position, which indicates the specimens are almost ideally thin for
49 EELS. Both deconvoluted and original EELS contain a high level of noise. Therefore, a
50 Lorentzian based least-squares regression analysis has been applied to fit the plasmon peak.
51
52
53
54
55
56
57
58
59
60

1
2
3
4
5
6
7
8
9
10
11
12
13
14
15
16
17
18
19
20
21
22
23
24
25
26
27
28
29
30
31
32
33
34
35
36
37
38
39
40
41
42
43
44
45
46
47
48
49
50
51
52
53
54
55
56
57
58
59
60

Figure 1(b) depicts the processed low-loss EELS of $In_{0.54}Ga_{0.46}N$ thin film, and the peak position E_{max} can be obtained with sufficiently high accuracy. Figure 1(c) demonstrates how the plasmon peak evolves and shifts from pure GaN, over two different ternary InGaN alloys, to pure InN.

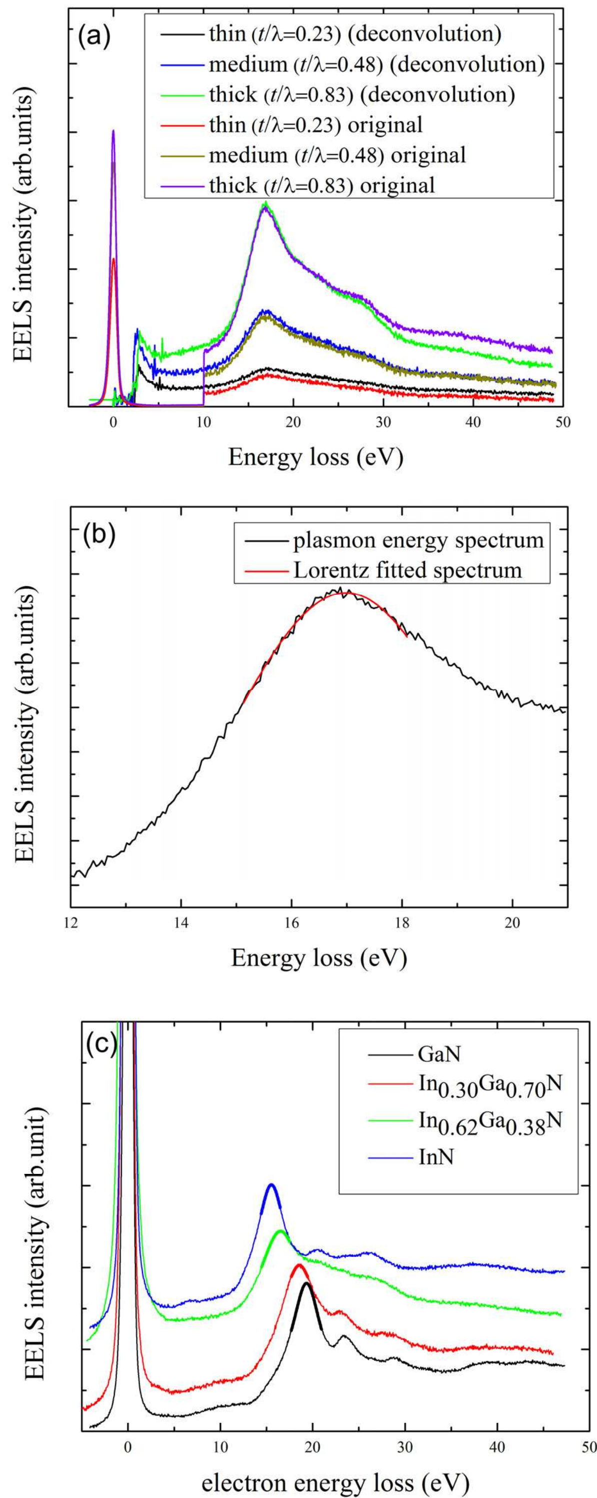

Figure 1: (a) comparison of original and deconvoluted EELS spectrum of $In_{0.54}Ga_{0.46}N$ thin

1
2
3
4
5
6
7
8
9
10
11
12
13
14
15
16
17
18
19
20
21
22
23
24
25
26
27
28
29
30
31
32
33
34
35
36
37
38
39
40
41
42
43
44
45
46
47
48
49
50
51
52
53
54
55
56
57
58
59
60

film (t/λ =0.23, 0.48, 0.83 where λ denotes the inelastic mean free path). (b) Lorentz curve fitted to central plasmon peak for $In_{0.54}Ga_{0.46}N$ sample with t/λ=0.83. (c) Comparison of plasmon peak shift from pure GaN, over two ternary InGaN alloys, to pure InN demonstrates how the peaks evolve. Raw data are displayed and the regions for the optimal Lorentz fits are highlighted in bold.

The EELS experiments were repeated three times for each specimen, using different specimen thicknesses. Then, a weighted average energy was calculated (the ideal specimen thickness for optimal signal-to-noise ratio in an EELS for a single plasmon excitation is given by $t=\lambda$). Table 1 shows the weighted average values of plasmon peak energies for different nominal indium concentrations.

nominal indium concentration, $x_{nominal}$	weighted average plasmon peak energy (eV)
0	19.33±0.01
0.135	18.69±0.04
0.20	18.42±0.01
0.30	18.27±0.01
0.40	17.66±0.05
0.54	17.00±0.02
0.62	16.76±0.04
0.74	16.14±0.03
0.84	15.88±0.02
1	15.52±0.01

Table 1: weighted average value of plasmon peak energy as function of nominal indium concentration

As the nominal concentration provided by the growers seemed not reliable, we used an additional EDXS analysis to check the indium concentration for each sample. For sufficiently thin samples, the Cliff-Lorimer k-factor provides a useful approach to determine the indium concentration of a thin film. For thicker specimens, either an additional absorption factor needs to be included or a thickness-dependent $k^*_{In,Ga}$ factor be defined which effectively includes absorption and fluorescence effects if the above intensities are recorded from thicker specimen regions [22].

$$k*_{In,Ga} = \frac{x\, I_{Ga}\, A_{In}}{(1-x)\, I_{In}\, A_{Ga}} \quad (1)$$

where $k^*_{In,Ga}$ is the effective k-factor for weight percent of the In L-line with respect to a Ga line (K or L), x is the indium concentration, I_{Ga} and I_{In} are the intensities of Ga and In lines, respectively, and A are the atomic weights of the corresponding elements.
We have performed Monte Carlo simulations for X-ray generation and detection using the CASINO code [23] to calculate theoretical $k^*_{In,Ga}$ values and to compare them to our experiments.
For indium concentrations x>0.5, simulations suggest the experimental curves of $k^*_{In,Ga}$ vs. Ga K/L ratio should be similar and ideally equal to the theoretical curve. By using the modeled

$k^*_{In,Ga}$ curves and experimental intensities I_{Ga} and I_{In}, a new indium concentration x can be obtained from equation (2). Then the $k^*_{\mathrm{In,Ga}}$ simulation is repeated for this updated indium concentration x to provide an updated value for $k^*_{\mathrm{In,Ga}}$, etc. If this is iterated, then the solution for each spectral measurement converges to exactly one combination of $k^*_{\mathrm{InL,GaL}}$, $k^*_{\mathrm{InL,GaK}}$ and x, yielding a self-consistent solution for quantification using Ga L or Ga K lines.

$$x = \frac{1}{1+\frac{I_{Ga}*A_{In}}{I_{In}*A_{Ga}*k^*_{InGa}}} \tag{2}$$

Figure 2 plots the new calibrated indium concentration versus the nominal concentration.

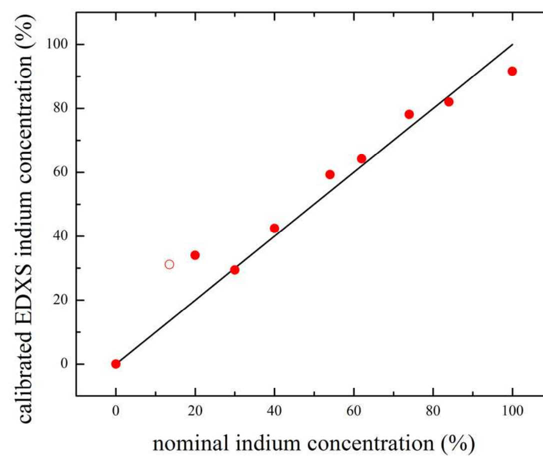

Figure 2: new calibrated indium concentration versus nominal indium concentration. For one sample only (marked by an open symbol) the iteration did not converge properly for both GaL and GaK line quantification, and the intensity ratio of Ga K/L was lower than modeled so this point has been excluded from further analysis.

We did not observe any strain effects on the plasmon peak position, as could be expected for biaxially strained thin quantum wells, however, for strained InGaN layers only a few nanometers thin it is almost impossible to disentangle the effects of strain and compositional gradients [24] and our layers were much thicker and partially relaxed.

The relationship between plasmon peak energy and this newly determined indium concentration is shown in figure 3. The relationship between plasmon peak energy and indium content is linear and can be expressed as

$$E_{max}[\mathrm{eV}] = (19.39\pm0.06) - (4.02\pm0.11)x$$

where x is the indium concentration and E_{max} is the plasmon peak energy. The adjusted R^2 (R^2=0.9845) confirms the plasmon peak energy versus calibrated indium concentration is linear over the complete compositional range $0<x<1$, with an uncertainty in the indium concentration (random mean-square error from linear regression) of $\Delta x=\pm0.037$, which indicates an improved accuracy in the determination of indium concentration of InGaN compared to previous studies [3].

1
2
3
4
5
6
7
8
9
10
11
12
13
14
15
16
17
18
19
20
21
22
23
24
25
26
27
28
29
30
31
32
33
34
35
36
37
38
39
40
41
42
43
44
45
46
47
48
49
50
51
52
53
54
55
56
57
58
59
60

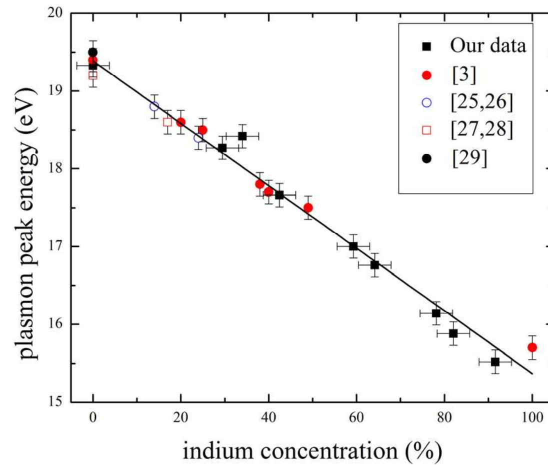

Figure 3: dependence of plasmon peak position on measured indium concentration in InGaN, including our data as well as data from other groups [3, 25-29]. The black line is the linear least-squares regression fit to all data.

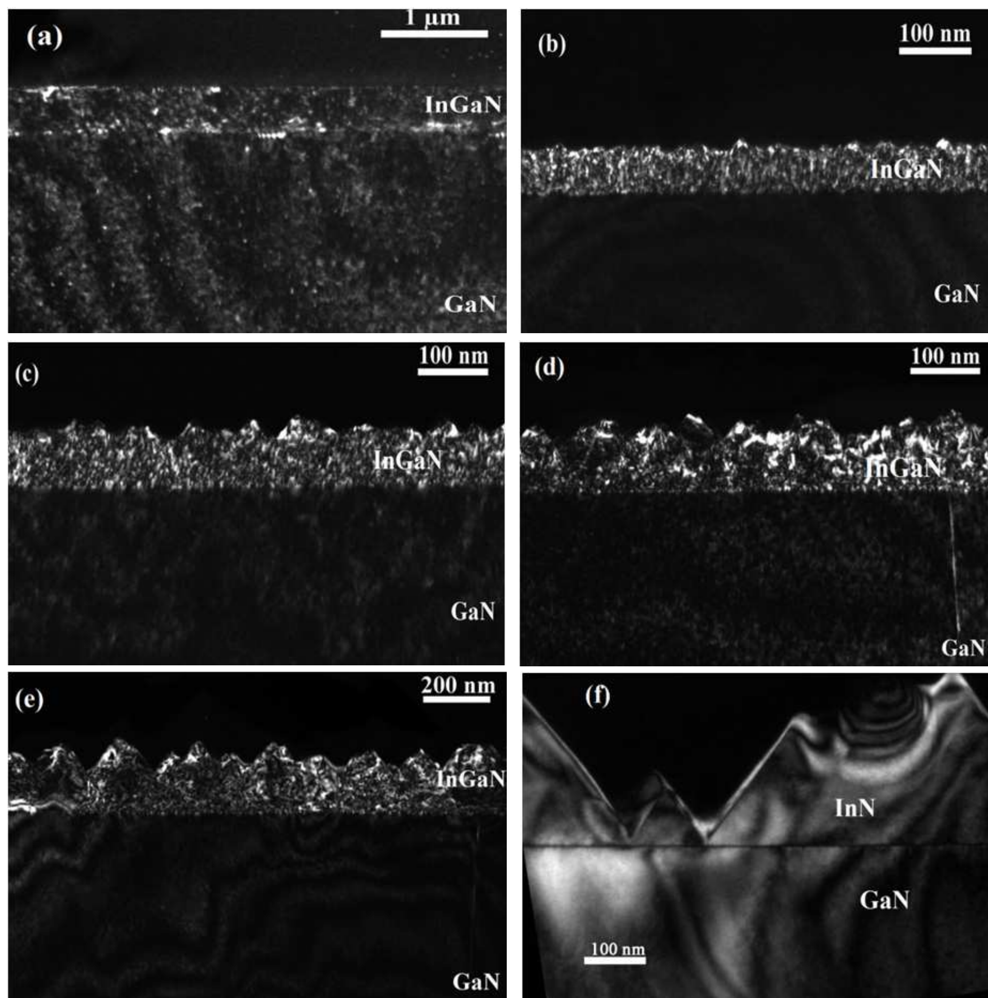

Figure 4: $\underline{\boldsymbol{g}}$=0002 weak beam image of (a) $In_{0.34}Ga_{0.66}N$, (b) $In_{0.42}Ga_{0.58}N$, (c) $In_{0.59}Ga_{0.41}N$, (d) $In_{0.64}Ga_{0.36}N$, (e) $In_{0.78}Ga_{0.22}N$, (f) $In_{0.92}Ga_{0.08}N$ (InN).

1 2 3 4 5 6 7 8 9 10 11 12 13 14 15 16 17 18 19 20 21 22 23 24 25 26 27 28 29 30 31 32 33 34 35 36 37 38 39 40 41 42 43 44 45 46 47 48 49 50 51 52 53 54 55 56 57 58 59 60

The increase of the indium concentration in InGaN quantum wells often leads to the formation of V-type defects [30]. Denser V-type defect formation will lead to a higher level of surface roughness. Figure 4 shows some ***g***=[0002] weak beam overview images of the different indium concentration samples investigated in the present study. From the investigation, it has been noticed that for low indium concentration ($x<0.3$), even 400nm thick films of InGaN have a smooth surface (see fig. 4a). When the indium concentration increases, the surface roughness increases dramatically and layer crystalline quality degrades as shown in figures 4 (b)-(e). However, for pure InN growth on GaN, the thin film is approximately 100-300nm thick and consists of facetted islands of pyramidal forms, as shown in figure 4 (f), but it exhibits a perfect crystalline quality, in contrast to the In rich ternary alloys.

4. Conclusion

We have studied the influence of indium content, x, of $In_xGa_{1-x}N$ thin films on EELS plasmon peak energy over the whole compositional range $0<x<1$. Our study confirms that the plasmon peak energy has a linear relationship on the indium concentration in the InGaN ternary system. By a combination of plasmon peak energy fitting and EDXS as a calibration tool to check the nominal indium content, the reliability in determination of the absolute indium concentration from EELS has been improved to $\Delta x=0.037$.

Acknowledgements

The investigated samples have been provided through the consortium of the EU project under contract N°: PITN-GA-2008-213238 (RAINBOW). MPC and PR acknowledge the EU for financial support and AIXTRON for growing the samples.

References

[1] Cheong MG, Suh E–K and Lee HJ 2002 Properties of InGaN/GaN quantum wells and blue light emitting diodes. *Journal of Luminescence* **99** 265-272.

[2] Galtrey MJ, Oliver RA, Kappers MJ, Humphreys CJ, Stokes DJ, Clifton PH and Cerezo A 2007 Three-dimensional atom probe studies of an $In_xGa_{1-x}N$/GaN multiple quantum well structure: assessment of possible indium clustering. *Appl. Phys. Lett.* **90** 061903.

[3] Kong X, Albert S, Bengoechea-Encabo A, Scanchez-Garcia MA, Calleja E and Trampert A 2012 Plasmon excitation in electron energy-loss spectroscopy for determination of indium concentration in (In,Ga)N/GaN nanowires. *Nanotechnology* **23** 485701.

[4] Y Narukawa, Y Kawakami, M Funato, S Fujita, S Fujita and S Nakamura 1997 Role of self-formed InGaN quantum dots for exciton localization in the purple laser diode emitting at 420 nm. *Appl. Phys. Lett.* **70** 981-983.

[5] Watanabe K, Nakanishi N, Yang JR, Inoke K, Hsu JT and Shiojiri M 2003 Atomic-scale strain field and In atom distribution in multiple quantum wells of InGaN/GaN. *Appl. Phys. Lett.* **82** 715-717.

[6] Vermaut P, Ruterana P, Nouet G, Salvador A, Botchkarev A, Sverdlov B and Morkoç H 1995 Microstructure of GaN epitaxially grown on hydrogen plasma cleaned 6H-SiC substrates. *Inst. Phys. Conf. Ser.* **146** 289-292.

[7] Ning XJ, Chien FR, Pirouz P, Yang JW and Khan MA 1996 Growth defects in GaN films on sapphire: the probable origin of threading dislocations. *J. Mater. Res.* **3** 580-592.

[8] Potin V, Ruterana P, Nouet G, Pond RC and Morkoç H 2000 Mosaic growth of GaN on (0001) sapphire : a high resolution electron microscopy and crystallographic study of dislocations from low angle to high angle grain boundaries. *Phys. Rev. B.* **61** 5587-5599.

[9] Potin V, Ruterana P and Nouet G 2000 HREM study of stacking faults in GaN layers grown on sapphire substrate. *J. Phys. Condensed Matter.* **12** 10301-10306.

[10] Smith DJ, Chandrasekhar D, Sverdlov B, Botchkarev A, Salvador A and Morkoc H 1995 *Appl. Phys. Lett.* **67** 1830-1832.

[11] Ruterana P, Barbaray B, Béré A, Vermaut P, Hairie A, Paumier E, Nouet G, Salvador A, Botchkarev A, and Morkoc H 1999 Formation and stability of the {11-20} stacking fault atomic configurations in wurtzite (Al,Ga,In) nitrides. *Phys. Rev. B* **59**, 15917-15925.

[12] Romano LT, Northrup JE and O'Keefe MA 1996 Inversion domains in GaN grown on sapphire. *Appl. Phys. Lett.* **69** 2394-2396.

[13] Potin V, Nouet G and Ruterana P 1999 Evidence for multiple atomic structure for the {10-10} inversion domain boundaries in GaN layers. *Appl. Phys. Lett.* **74** 947-949.

[14] McCluskey MD, Romano LT, Krusor BS, Bour DP and Johnson NM 1998 Phase separation in annealed InGaN/GaN multiple quantum wells. *Appl. Phys. Lett.* **72** 1730-1732.

[15] Ruterana P, Nouet G, Van der Stricht W, Moerman I and Considine L 1998 Chemical ordering in wurtzite $In_xGa_{1-x}N$ layers grown on (0001) sapphire by metalorganic vapor phase epitaxy. *Appl. Phys. Lett.* **72** 1742-1744.

[16] Walther T, Wolf F, Recnik A and Mader W 2006 Quantitative microstructural and spectroscopic investigation of inversion domain boundaries in sintered zinc oxide ceramics doped with iron oxide. *Int. J. Mat. Res.* **97** 934-942.

[17] Potapov PL and Schryvers D 2004 Measuring the absolute position of EELS ionisation edges in a TEM. *Ultramicroscopy* **99** 73-85.

[18] Walther T and Humphreys CJ 1999 A quantitative study of compositional profiles of chemical vapour-deposited strained silicon-germanium/ silicon layers by transmission electron microscopy. *J. Crystal Growth* **197** 113-128.

[19] Amari H, Zhang HY, Geelhaar L, Chèze C, Kappers MJ and Walther T 2011 Nanoscale EELS analysis of elemental distribution and band-gap properties in AlGaN epitaxial layers, Proc. 17th Intern. Conf. on Microscopy of Semiconducting Materials, Cambridge (eds. Walther T and Midgley P A). *Journal of Physics Conference Series* **326** 012039.

[20] Amari H, Kappers MJ, Humphreys CJ, Chèze C and Walther T 2012 Measurement of the Al content in AlGaN epitaxial layers by combined energy-dispersive X-ray and electron energy-loss spectroscopy in a transmission electron microscope. *Physica Status Solidi C* **9** 1079-1082.

[21] Egerton RF, Williams BG and Sparrow TG 1985 Fourier deconvolution of electron energy-loss spectra. *Proc. R. Soc.* London A **398** 395-404.

[22] Walther T 2010 An improved approach to quantitative X-ray microanalysis in (S)TEM: thickness dependent *k*-factors. *Journal of Physics Conference Series* **241** 012016.

[23] Hovington P, Drouin D and Gauvin R 1997 CASINO: a new Monte Carlo code in C language for electron beam interactions. 1. Description of the program. *Scanning* **19** 1-14.

[24] Keast VJ, Sharma N and Humphreys CJ 2001 Proc. 12th Microscopy of Semiconducting Materials Conference, Oxford. Inst. Phys. Conf. Ser. **169** 259-262.

[25] Jinschek JR, Erni R, Gardner NF, Kim AY and Kisielowski C 2006 Local indium segregation and band gap variations in high efficiency green light emitting InGaN/GaN diodes. *Solid State Commun.* **137** 230-234.

[26] Bosman M, Tang LJ, Ye JD, Tan ST, Zhang Y and Keast VJ 2009 Nanoscale band gap spectroscopy on ZnO and GaN-based compounds with a monochromatic electron microscope. *Appl. Phys. Lett.* **95** 101110.

[27] Egerton RF 2009 Electron energy-loss spectroscopy in the TEM. *Rep. Prog. Phys.* **72** 016502.

[28] Specht P, Ho JC, Xu X, Armitage R, Weber ER, Erni R and Kisielowski C 2006 Zincblende and wurtzite phases in InN epilayers and their respective band transitions. *J. Cryst. Growth.* **288** 225-229.

[29] Specht P, Xu X, Armitage R, Weber ER, Erni R and Kisielowski C 2006 Local band and defect transitions in InGaN observed by valence electron energy loss spectroscopy. *Physica B* **376/377** 552-555.

[30] Wu XH, Elsass CR, Abare A, Mack M, Petroff PM, Denbaars SP and Speck JS 1998 Structural origin of V-defects and correlation with localized excitonic centers in InGaN/GaN multiple quantum wells. *Appl. Phys. Lett.* **72** 692-694.